Research Article

Journal of Environmental Nanotechnology

Facile Solvothermal Synthesis and Characterization Studies of Pure and Lead-doped Cadmium Sulfide Nanoparticles for Potential Photovoltaic Applications

P. Gowdhaman, R. Sakthi Sudar Saravanan, Haresh M. Pandya*
Department of Physics, Chikkanna Government Arts College, Tirupur, TN, India
Received: 08.12.2020 Accepted: 18.01.2021 Published: 30-01-2021
*haresh.pandya@rediffmail.com

ABSTRACT

Pure and Pb-doped Cadmium Sulfide (CdS) nanoparticles were synthesized using a straight forwarded solvothermal technique. The powder X-ray diffraction (PXRD) studies done on the sample synthesized revealed the wurtzite phase of nanoparticles with improved crystalline properties due to the integration of dopant Pb into the host CdS. The UV-Vis characterization studies also reveal enhanced optical properties of the nanoparticles, which can be efficiently tapped for various photovoltaic applications.

Keywords: Cadmium sulfide nanoparticles; Doped CdS; Photovoltaic; Quantization effect; Solvothermal synthesis.

1. INTRODUCTION

In recent years, there has been considerable interest generated in the study of compound semiconductors with dimensions in the nanometer range. The novel optical and transport properties exhibited by these materials continuously fascinate and hold the interest of researchers worldwide. Over the last 10 years, it has been realized that nanomaterials have some unique properties, which have been attributed to their size-dependent bandgap energy (Khan *et al.* 2019b; Iqbal *et al.* 2020). Nano-semiconductor materials that exhibit peculiar properties which are rarely shown by their bulk counterparts have attracted much interest from both fundamental and technological researchers (Barglik-Chory *et al.* 2003; Priya *et al.* 2012; Loudhaief *et al.* 2018).

Metal oxide and metal sulfide semiconductor nanoparticles in their pure and doped form were synthesized and examined widely due to their intervening properties, which makes them attractive to the material scientists for their countless applications (Martínez-Alonso *et al.* 2014; Malashchonak *et al.* 2015; Ertis *et al.* 2017; Khan *et al.* 2019a). Among many combinations of these materials, pure and doped metal sulfides of group II – VI elements are particularly under the limelight of researchers. These semiconductor materials have greater scope in the research arena and are not limited to solar photovoltaic (Priya *et al.* 2012; Martínez-Alonso *et al.* 2014; Veerathangam *et al.* 2018), photocatalytic (Chauhan *et al.* 2013; Ertis *et al.* 2017), energy materials, storage devices, biomedical engineering materials, etc. Cadmium sulfide (CdS) is one such metal sulfide semiconductor with enormous potential applications as it can be easily doped with other elements thus exhibiting a wide range of optical and electrical properties. In doped CdS semiconductors, the impurity states play a crucial role in affecting the electronic energy structures and transition probabilities in contrast with undoped ones (Nag *et al.* 2008). For doped nanocrystalline semiconductors, quantum confinement effects in the energy states produce unusual physical and optical behavior (Maleki *et al.* 2007; Nag *et al.* 2008; Priya *et al.* 2012; Malashchonak *et al.* 2015). The doping ions act as recombination centers for the excited electron-hole pairs resulting in a display of a strong and characteristic luminescence (Barglik-Chory *et al.* 2003; Chauhan *et al.* 2013; Qi *et al.* 2015; Khan *et al.* 2019b; Khan *et al.* 2019a; Iqbal *et al.* 2020).

Arya *et al.* have prepared Cu-doped CdS nanoparticles via the sol-gel method and utilized it as a photodiode (Arya *et al.* 2018). Ag-doped CdS nanoparticles were synthesized by Iqbal and his team using the chemical co-precipitation method (Iqbal *et al.* 2020). They claim that these nanoparticles are suitable for solar cell-specific applications due to their reduced bandgap and increased optical transparency. Chauhan *et al.* used Fe-doped CdS (Chauhan *et al.* 2013), and Ertis and his team used different metal ion (Ni, Co, Ce, Sb) doped CdS nanoparticles (Ertis *et al.* 2017) for the photodegradation of methylene blue under visible light

irradiation and found it to be useful for the same. Likewise, many other research groups have investigated the CdS nanoparticles doped with Mn (Barglik-Chory *et al.* 2003; Nag *et al.* 2008; Kim *et al.* 2018), La (Qi *et al.* 2015), Bi (Loudhaief *et al.* 2018), Gd (Khan *et al.* 2019a) and studied the properties of these materials for applications not limited to solar energy conversion (Martínez-Alonso *et al.* 2014; Qi *et al.* 2015; Veerathangam *et al.* 2018; Kim *et al.* 2018; Khan *et al.* 2019b), photocatalytic degradation (Chauhan *et al.* 2013), photodiode (Arya *et al.* 2018) and optoelectronic (Priya *et al.* 2012; Manthrammel *et al.* 2018; Khan *et al.* 2019a) device applications. More recently, Khan *et al.* have theoretically explored the optical properties of the Pb-doped CdS system by interpreting computational modeling (Khan *et al.* 2019b). They have suggested that Pb enhances the optoelectrical properties of CdS lattice, and hence it can be labeled as an ideal material for photo-detector, quantum dot-based solar cells and photosensitive applications. Many research articles have reported the synthesis of pure and doped CdS nanoparticles whereas, literature on the experimental study of Pb-doped CdS nanoparticles and their properties are inadequately reported. Hence, an attempt has been made in this research article to highlight the peculiar and fascinating experimental properties of Pb-doped CdS nanoparticles.

As for CdS nanoparticles and their doping is a concern, plenty of synthesis procedures with special emphasis on key parameters have been reported to enable and fine-tune physical, chemical and optical properties of semiconductors. For example, thermal decomposition (Martínez-Alonso *et al.* 2014), laser ablation, microwave irradiation (Nabiyouni *et al.* 2013; Martínez-Alonso *et al.* 2014; Manthrammel *et al.* 2018), sonochemical (Martínez-Alonso *et al.* 2014), reverse micelles process, chemical reduction, co-precipitation method (Manthrammel *et al.* 2018; Iqbal *et al.* 2020), ultrasonic irradiation, radiolysis, solvothermal (Li *et al.* 1999; Priya *et al.* 2012; Martínez-Alonso *et al.* 2014) and electrochemical etc. In most of the above papers controlling the particle size distribution and stability has been reported to be difficult. Taking the above considerations into mind, in the present work, an attempt has been made to synthesize and characterize pure and two different concentrations of Pb^{2+} doped (4 mole% and 8 mole%) CdS nanoparticles by using one of the convenient and cost-effective simple solvothermal methods to obtain high-quality uniform size nanoparticles. The structural and optical properties of these nanoparticles have also been analyzed for their suitability in photovoltaic applications.

2. EXPERIMENTAL DETAILS

2.1 Synthesis and Characterization of Pure and Pb-doped CdS nanoparticles

A facile solvothermal technique was adopted for the synthesis of pure and Pb-doped CdS nanoparticles using a conventional heating technique. An equal proportion of metal-bearing precursor cadmium acetate dihydrate ($(CH_3COO)_2Cd.2H_2O$) and sulfur bearing precursor thiourea (CH_4N_2S) was dissolved in 300 ml of ethylene glycol and stirred well to obtain a clear solution and then heated at 200 ºC using a hot plate until the solvent evaporated completely. The final colloidal precipitate obtained was washed with double distilled water and acetone several times and filtered to obtain the final product. For the synthesis of Pb-doped (4 and 8 mole %) CdS nanoparticles, the desired proportion of lead acetate trihydrate was added separately to the homogeneous solution of reactants and stirred for an hour. The final product was collected and characterized structurally and optically. Structural characterization was carried out using powder X-ray diffraction (Panalytical X'PERT PRO). The morphology of these nanoparticles was analyzed using a field emission scanning electron microscope (TESCAN-MIRA3 XMU) and a UV-Vis Spectrometer (Shimadzu-UV 3600Plus) was used to analyze the optical properties of these nanoparticles.

3. RESULTS AND DISCUSSIONS

3.1 Structural Analysis

The obtained X-ray diffraction patterns (XRD) of pure CdS, 4 mole% Pb^{2+} and 8 mole% Pb^{2+} doped CdS nanoparticles are shown in Fig. 1. The diffraction peaks (1 0 0), (0 0 2), (1 0 1), (1 0 2), (1 1 0), (1 0 3), (1 1 2), (0 0 4) and (2 0 3) indicate that the synthesized pure and Pb-doped CdS nanoparticles have wurtzite structure, from which the observed peaks can be indexed to the hexagonal phase of CdS with space group $P6_3mc$. In comparison to JCPDS file No. 41-1049, the peak orientations from the spectra showed the hexagonal structure of the pure and Pb-doped CdS (Maleki *et al.* 2007; Priya *et al.* 2012; Nabiyouni *et al.* 2013; Abd El-Sadek *et al.* 2019).

From the recorded spectra, one can infer that crystallinity improves with the increasing concentration of dopant in the host CdS lattices. More interestingly, when Pb^{2+} was added into the pure CdS, no diffraction peaks corresponding to PbS/CdO were observed in the XRD pattern. It was also observed that the broadening of diffraction peaks was slightly decreased. In addition, a minor increase in peak intensity was observed in Fig. 1. It was observed that the substitution of Pb in the CdS

lattice results in a slight increase in the volume of the unit cell, thereby producing a change (enhancement in a and c directions) in the lattice parameters as inferred by the shift in X-ray diffraction peak to the high angle side.

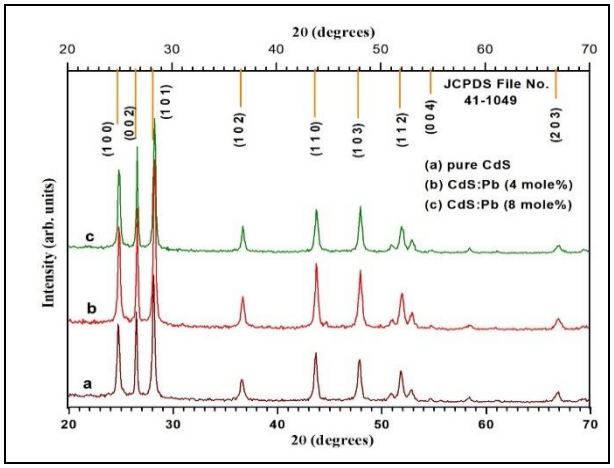

Fig. 1: X-ray diffractograms of pure CdS, 4 mole% Pb^{2+} and 8 mole% Pb^{2+} doped CdS nanoparticles.

The lattice parameters (a=b, c) of the CdS nanoparticles are calculated from the following equation,

$$\frac{1}{d^2} = \frac{4}{3}\left(\frac{h^2+hk+k^2}{a^2}\right) + \frac{l^2}{c^2}$$

where, d is the inter-planar distance and h, k, l are the Miller indices of the respective plane. The observed structural data from the XRD measurements are summarized in Table 1.

Table 1. The observed structural data from XRD measurements

Sample Name	Calculated parameters			Crystallite size, nm
	a=b (Å)	c (Å)	Volume (Å^3)	
CdS (JCPDS File No. 41-1049)	4.207	6.843	104.89	-
Pure CdS	4.193	6.816	103.78	14.3
4 mole% Pb doped CdS	4.214	6.836	105.13	15.7
8 mole% Pb doped CdS	4.226	6.847	105.89	18.3

The crystallite sizes (D) of the pure CdS, 4 mole% Pb^{2+} and 8 mole% Pb^{2+} doped CdS nanoparticles are estimated from XRD pattern by using the Scherer equation (Abd El-Sadek *et al.* 2019),

$$D = \frac{0.9\lambda}{\beta \cos\theta}$$

where, D is the mean size (diameter) of the crystallite, β is the full width at half maximum of intensity (in radians), λ is the wavelength of the X- ray radiation used (1.540598 AU), and θ is half the angle at which maximum intensity was observed. The estimated crystallite size of prepared nanoparticles is given in Table 1 and it indicates the nanocrystalline nature of the samples. Also, the crystallite sizes of 4 and 8 mole% Pb^{2+}-doped CdS nanoparticles are larger than that of pure CdS and are found to increase with the increase in dopant concentration. The large atomic radius of Pb is one of the factors that contribute to the increase in the crystallite size of these nanoparticles. This reveals the incorporation of Pb^{2+} into the host CdS matrix.

3.2 FESEM Analysis

The field emission scanning electron microscopic structures of pure CdS and 8 mole% Pb^{2+}-doped CdS nanoparticles are shown in Fig. 2. From the FESEM microstructures, it can be seen that the pure CdS nanoparticles are composed of nanoparticles with a diameter of 25 to 35 nm, which is consistent with the values calculated by Scherrer's formula. It can also be seen that the Pb^{2+} doping in CdS matrices has only a little influence on the morphology of the nanocrystals. However, particle size increases with the addition of dopants in the CdS lattices. The estimated particle size for 8 mole % Pb doped CdS nanoparticles is 40-50 nm. Thus, it appears to be very big in size as compared to pure CdS nanoparticles.

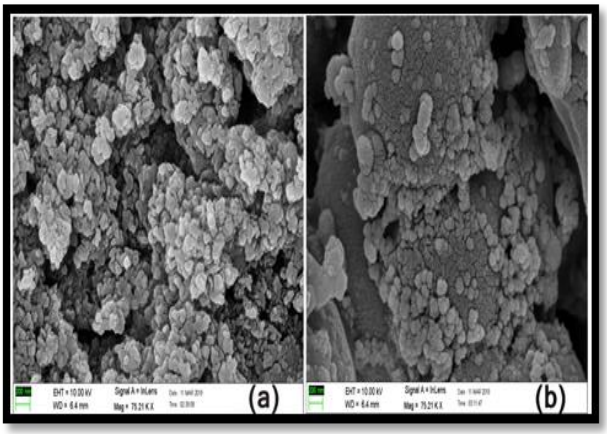

Fig. 2: FESEM microstructures of solvothermal synthesized (a) pure CdS nanoparticles, (b) 8 mole% Pb^{2+}-doped CdS nanoparticles

3.3 UV-Vis. Analysis

The variation of absorbance as a function of incident photon wavelength (λ) for nanocrystalline pure CdS and different concentrations of Pb^{2+} (4 mole % and 8 mole %) doped CdS nanoparticles are shown in Fig. 3a. The corresponding incident photon energy (hυ) vs. $(\alpha h\upsilon)^2$ plot is given in Fig. 3b. The absorption spectra of pure and doped CdS nanoparticles consist of short wavelength tail bands. This reveals that the particle size distribution is narrow. The increase in absorption intensity is due to the increasing concentration of Pb^{2+} dopant from 4 mole % to 8 mole % in the host CdS lattices.

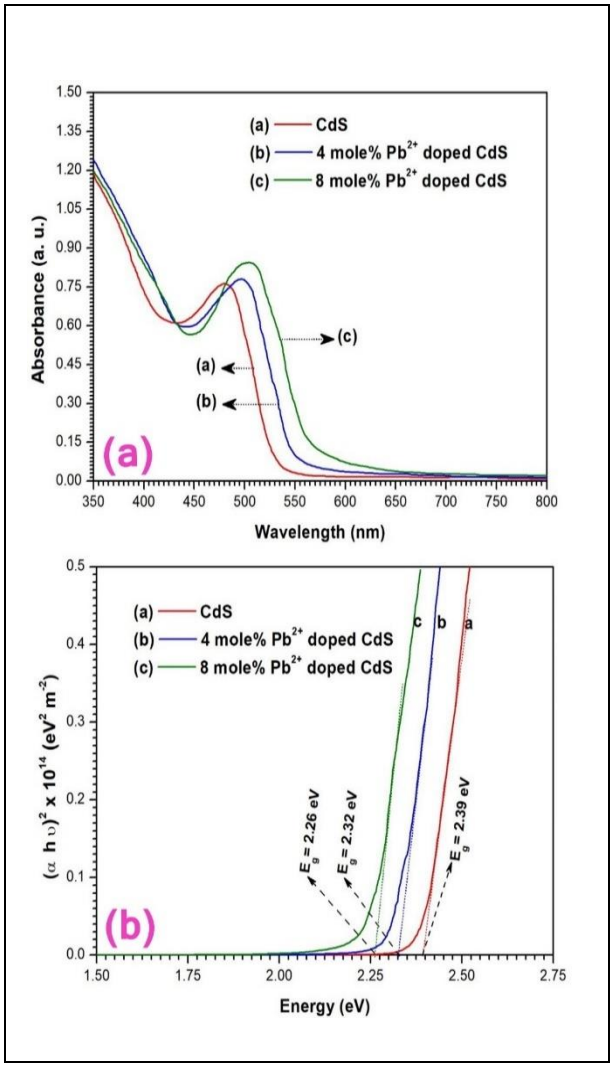

Fig. 3: (a) UV-Vis Absorbance spectra and (b) Optical bandgap measurement plots of pure and doped CdS nanoparticles

The fundamental absorption edge in most semiconductor nanoparticles follows an exponential law. The absorption coefficient has been reported to obey the following equation (Saravanan *et al.* 2012):

$$(\alpha h\upsilon)^{1/n} = A(h\upsilon - E_g)$$

where, υ is the frequency of the incident beam), A is a constant, E_g is the optical band gap and n is an exponent which can be assumed to have values of $^1/_2$, $^3/_2$, 2 and 3 depending on the nature of electronic transition responsible for the absorption: $n=^1/_2$ for allowed direct transition, $n=^3/_2$ for forbidden direct transition, n=2 for allowed indirect transition and n=3 for forbidden indirect transition. The present system of pure and doped CdS semiconductor nanoparticles obeys the role of direct transition. The relation between the optical gap, optical absorption coefficient (α) and the energy (hυ) of the incident photon is given by (Saravanan *et al.* 2012),

$$(\alpha h\upsilon)^2 = A(h\upsilon - E_g)$$

The calculated optical band gap (E_g) for pure CdS, 4 mole % Pb-doped CdS and 8 mole % Pb-doped CdS nanoparticles was calculated to be 2.39 eV, 2.32 eV and 2.26 eV, respectively. It is evident from the energy bandgap determination spectra that the value of E_g decreases with the addition of Pb^{2+} in the host CdS lattices and decreases with the increase of dopant concentration from 4 mole % to 8 mole %. This may be ascribed to the growth in grain size and growth in density of defect states.

4. CONCLUSIONS

Pure and doped CdS nanoparticles were synthesized successfully using a facile solvothermal process. The diffraction peaks obtained from X-ray diffraction patterns (XRD) of pure CdS, 4 mole % Pb^{2+} and 8 mole % Pb^{2+} doped CdS nanoparticles were found to have preferential orientations along (1 0 0), (0 0 2), (1 0 1), (1 0 2), (1 1 0), (1 0 3), (1 1 2), (0 0 4) and (2 0 3) plane, from which the observed peaks can be indexed to hexagonal phase of CdS with space group $P6_3mc$. Further, from the recorded spectra, one can understand that the degree of crystallinity improves with the increasing concentration of dopant in the host CdS lattices. More interestingly, when Pb^{2+} is added into the pure CdS, no diffraction peaks corresponding to PbS/CdO have been observed in the XRD pattern. However, the broadening of the peak has slightly decreased, whereas the peak intensity has increased. Thus the lattice parameters and volume of the unit cell are slightly increased. This reveals that the Pb^{2+} ions are well incorporated within the host matrix. The estimated crystallite size of the Pb^{2+}-doped CdS nanoparticles is larger than that of pure CdS nanoparticles, which can be

attributed to the higher ionic radii of Pb than that of parent CdS.

From the FESEM microstructures, it can be seen that the pure CdS nanoparticles are composed of nanoparticles with a diameter 25 to 35 nm and the particle size increases to 40-50 nm with the addition of a dopant (8 mole % Pb) in the CdS lattices. The calculated optical band gap (E_g) for pure CdS, 4 mole % Pb-doped CdS and 8 mole % Pb-doped CdS nanoparticles are found to be 2.39 eV, 2.32 eV and 2.26 eV, respectively.

The significant difference between the bandgap values of pure and doped nanoparticles is evidence for incorporating dopants in the parent CdS lattices. Further, the bandgap of these nanoparticles can be tuned well with a selection of suitable methods for synthesis. The solvothermal method leads to the agglomeration of particles due to the direct heating procedure. Undoubtedly, the prepared pure and doped CdS nanoparticles synthesized by the simple solvothermal method yielded promising results without any additional impurities. A disadvantage of the present solvothermal method that we have observed is that the crystallite size over 10 nm obtained in the samples limits their applications due to the lack of the size quantization effect. The authors observed that a suitable futuristic method with pronounced control over crystallite size would open up new vistas for these synthesized materials.

FUNDING

This research received no specific grant from any funding agency in the public, commercial, or not-for-profit sectors.

CONFLICTS OF INTEREST

The authors declare that there is no conflict of interest.

COPYRIGHT

REFERENCES

Abd El-Sadek, M. S., Wasly, H. S. and Batoo, K. M., X-ray peak profile analysis and optical properties of CdS nanoparticles synthesized via the hydrothermal method, *Appl. Phys., A* 125(4), 283 (2019). https://dx.doi.org/10.1007/s00339-019-2576-y

Arya, S., Sharma, A., Singh, B., Riyas, M., Bandhoria, P., Aatif, M. and Gupta, V., Sol-gel synthesis of Cu-doped p-CdS nanoparticles and their analysis as p-CdS/n-ZnO thin film photodiode, *Opt. Mater.*, 79, 115–119 (2018). https://dx.doi.org/10.1016/j.optmat.2018.03.035

Barglik-Chory, C., Remenyi, C., Dem, C., Schmitt, M., Kiefer, W., Gould, C., Rüster, C., Schmidt, G., Hofmann, D. M., Pfisterer, D. and Müller, G., Synthesis and characterization of manganese-doped CdS nanoparticles, *Phys. Chem. Chem. Phys.*, 5(8), 1639–1643 (2003). https://dx.doi.org/10.1039/b300343d

Chauhan, R., Kumar, A. and Chaudhary, R. P., Visible-light photocatalytic degradation of methylene blue with Fe doped CdS nanoparticles, *Appl. Surf. Sci.*, 270, 655–660 (2013). https://dx.doi.org/10.1016/j.apsusc.2013.01.110

Ertis, I. F., Boz, I., Synthesis and characterization of metal-doped (Ni, Co, Ce, Sb) CdS catalysts and their use in methylene blue degradation under visible light irradiation, *Mod. Res. Catal.*, 06(01), 01–14 (2017). https://dx.doi.org/10.4236/mrc.2017.61001

Iqbal, T., Ara, G., Khalid, N. R. and Ijaz, M., Simple synthesis of Ag-doped CdS nanostructure material with excellent properties, *Appl. Nanosci.*, 10(1), 23–28 (2020). https://dx.doi.org/10.1007/s13204-019-01044-y

Khan, A., Shkir, M., Manthrammel, M. A., Ganesh, V., Yahia, I. S., Ahmed, M., El-Toni, A. M., Aldalbahi, A., Ghaithan, H. and AlFaify, S., Effect of Gd doping on structural, optical properties, photoluminescence and electrical characteristics of CdS nanoparticles for optoelectronics, *Ceram. Int.*, 45(8), 10133–10141 (2019a). https://dx.doi.org/10.1016/j.ceramint.2019.02.061

Khan, M. J. I., Kanwal, Z., Usmani, M. N., Zeeshan, M. and Yousaf, M., An insight into optical properties of Pb:CdS system (a theoretical study), *Mater. Res. Express.*, 6(6), 65904 (2019b). https://dx.doi.org/10.1088/2053-1591/ab0abf

Kim, J.-Y., Jang, Y. J., Park, J., Kim, J., Kang, J. S., Chung, D. Y., Sung, Y.-E., Lee, C., Lee, J. S. and Ko, M. J., Highly loaded PbS/Mn-doped CdS quantum dots for dual application in solar-to-electrical and solar-to-chemical energy conversion, *Appl. Catal. B Environ.*, 227, 409–417 (2018). https://dx.doi.org/10.1016/j.apcatb.2018.01.041

Li, Y., Liao, H., Ding, Y., Fan, Y., Zhang, Y. and Qian, Y., Solvothermal elemental direct reaction to CdE (E = S, Se, Te) semiconductor nanorod, *Inorg. Chem.*, 38(7), 1382–1387 (1999). https://dx.doi.org/10.1021/ic980878f

Loudhaief, N., Labiadh, H., Hannachi, E., Zouaoui, M., Salem, M. and Ben, Synthesis of CdS nanoparticles by hydrothermal method and their effects on the electrical properties of bi-based superconductors, *J. Supercond. Nov. Magn.*, 31(8), 2305–2312 (2018). https://dx.doi.org/10.1007/s10948-017-4496-4

Malashchonak, M. V., Mazanik, A. V., Korolik, O. V., Streltsov, E. A. and Kulak, A. I., Influence of wide band gap oxide substrates on the photoelectrochemical properties and structural disorder of CdS nanoparticles grown by the successive ionic layer adsorption and reaction (SILAR) method, *Beilstein J. Nanotechnol.*, 6(1), 2252–2262 (2015). https://dx.doi.org/10.3762/bjnano.6.231

Maleki, M., Sasani Ghamsari, M., Mirdamadi, S. and Ghasemzadeh, R., A facile route for preparation of CdS nanoparticles, *Semicond. Physics, Quantum Electron. Optoelectron.*, 10(1), 30–32 (2007). https://dx.doi.org/10.15407/spqeo10.01.030

Manthrammel, M. A., Ganesh, V., Shkir, M., Yahia, I. S. and Alfaify, S., Facile synthesis of La-doped CdS nanoparticles by microwave assisted co-precipitation technique for optoelectronic application, *Mater. Res. Express.*, 6(2), 025022 (2018). https://dx.doi.org/10.1088/2053-1591/aaed9c

Martínez-Alonso, C., Rodríguez-Castañeda, C. A., Moreno-Romero, P., Coria-Monroy, C. S. and Hu, H., Cadmium sulfide nanoparticles synthesized by microwave heating for hybrid solar cell applications, *Int. J. Photoenergy.*, 2014, 01–11 (2014). https://dx.doi.org/10.1155/2014/453747

Nabiyouni, G., Azizi, E. and Nasrollahi, N., A simple microwave method for synthesis of CdS nanoparticles, *J. Clust. Sci.*, 24(4), 1043–1055 (2013). https://dx.doi.org/10.1007/s10876-013-0596-x

Nag, A., Sapra, S., Gupta, S. Sen, Prakash, A., Ghangrekar, A., Periasamy, N. and Sarma, D. D., Luminescence in Mn-doped CdS nanocrystals, *Bull. Mater. Sci.*, 31(3), 561–568 (2008). https://dx.doi.org/10.1007/s12034-008-0087-0

Priya, M., Saravanan, R. S. S. and Mahadevan, C. K., Novel Synthesis and characterisation of CdS nanoparticles, *Energy Procedia.*, 15, 333–339 (2012). https://dx.doi.org/10.1016/j.egypro.2012.02.040

Qi, X., Zou, X. and He, S., La doping of CdS for enhanced CdS/CdSe quantum dot cosensitized solar cells, *J. Chem.*, 2015, 01–07 (2015). https://dx.doi.org/10.1155/2015/710140

Saravanan, R. S. S., Pukazhselvan, D. and Mahadevan, C. K., Studies on the synthesis of cubic ZnS quantum dots, capping and optical–electrical characteristics, *J. Alloys Compd.*, 517, 139–148 (2012). https://dx.doi.org/10.1016/j.jallcom.2011.12.060

Veerathangam, K., Senthil Pandian, M. and Ramasamy, P., Photovoltaic performance of Pb-doped CdS quantum dots for solar cell application, *Mater. Lett.*, 220, 74–77 (2018). https://dx.doi.org/10.1016/j.matlet.2018.03.007